

## Pronounced stabilisation of the ferrocenium state of ferrocenecarboxylic acid by salt bridge formation with a benzamidine

Graeme Cooke,<sup>a,\*</sup> Florence M. A. Duclairoir,<sup>a</sup> Arno Kraft,<sup>a</sup> Georgina Rosair<sup>a</sup> and Vincent M. Rotello<sup>b</sup>

<sup>a</sup>Centre for Biomimetic Design and Synthesis, Chemistry, School of Engineering and Physical Sciences, Heriot-Watt University, Riccarton, Edinburgh EH14 4AS, UK

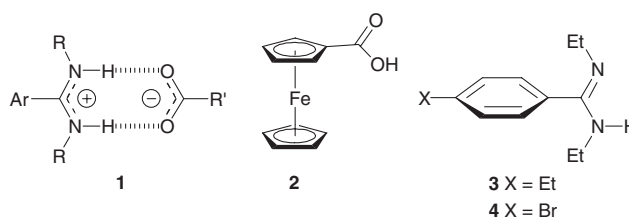
<sup>b</sup>Department of Chemistry, University of Massachusetts at Amherst, Amherst, MA 01002, USA

Received 14 August 2003; revised 13 October 2003; accepted 31 October 2003

**Abstract**—Salt bridge formation between ferrocenecarboxylic acid and an excess of a *N,N'*-diethylsubstituted benzamidine leads to a  $-0.27$  V shift in the half-wave potential of the ferrocene moiety, corresponding to a  $26 \text{ kJ mol}^{-1}$  stabilisation of the ferrocenium state.

© 2003 Elsevier Ltd. All rights reserved.

The development of hydrogen-bonded host–guest complexes with electrochemically controllable binding properties is a rapidly emerging field within supramolecular chemistry.<sup>1</sup> The electrochemically induced oxidation<sup>2</sup> or reduction<sup>2d,3</sup> of the components of a host–guest dyad can profoundly influence the electrostatic interactions between the complementary units, thereby affording systems with switchable binding properties. To date, only modest redox enhancement of binding efficiency has been observed for host–guest systems that are modulated by oxidative processes, whilst the largest levels of redox modulation are currently observed upon reduction of one of the components of the complex. However, one of the challenges to the eventual application of reduction-modulated host–guest assemblies is the instability of radical anions formed under aerobic conditions, as this limits the application of these systems to oxygen-free environments. Thus, the development of hydrogen-bonded systems with binding characteristics that can be significantly enhanced upon oxidation of one



or more of the components of the complex are important targets.

A large number of biological systems mediate their redox activity through proton transfer processes.<sup>4</sup> Salt bridges formed between a carboxylate and an unsubstituted amidine (e.g., **1**, R = H) have proved to be an attractive biomimetic system to investigate the mechanism of proton-coupled electron transfer in biological systems.<sup>5</sup> Here, we investigate the effect complex formation between ferrocenecarboxylic acid **2** and *N,N'*-diethyl-substituted benzamidines **3**<sup>6a,b</sup> or **4**<sup>6c</sup> has on the redox properties of the iron centre of **2**.<sup>5</sup> Substituted benzamidines **3** and **4** were chosen because their *N*-ethyl substituents suppress aggregation and impart solubility to the benzamidine and their corresponding complexes with ferrocenecarboxylic acid in nonpolar solvents (e.g.,  $\text{CHCl}_3$  or  $\text{CH}_2\text{Cl}_2$ ), where hydrogen bonding interactions

**Keywords:** Ferrocenecarboxylic acid; Amidine; Recognition; Electrochemistry.

\* Corresponding author. Fax: +44-131-451-3180; e-mail: [g.cooke@hw.ac.uk](mailto:g.cooke@hw.ac.uk)

between the complementary units are strong. Amidinium ferrocenecarboxylates **2**·**3** and **2**·**4** were obtained by dissolution of an equimolar mixture of the components in hot ethanol, followed by recrystallisation of the resulting 1:1 salt from hexane. The formation of a complex in  $\text{CDCl}_3$  was confirmed by  $^1\text{H}$  NMR spectroscopy.<sup>†</sup> The chemical shift of the NH signal of **2**·**3** observed at  $\delta_{\text{H}} = 12.8$ , is indicative of strong hydrogen bond formation. Both *N*-ethyl groups of the complexes gave rise to one triplet and quartet in their  $^1\text{H}$  NMR spectra, which is consistent with an (*E,E*)-configured amidine.<sup>6</sup> We note that the (*E,Z*) amidine isomer is preferred thermodynamically (and in polar solvents), but the absence of line broadening for the *N*-ethyl signals suggests that isomerisation of the amidine does not occur on the NMR time scale.

Further confirmation of the structure of the complex between **2** and **3** was provided by X-ray crystallography.<sup>‡</sup> Slow evaporation of a solution of the 1:1 salt in  $\text{CH}_2\text{Cl}_2$  gave crystals suitable for X-ray diffraction (Fig. 1). The crystal structure shows that two hydrogen bonds are formed between ferrocenecarboxylic acid **2** and (*E,E*)-configured benzamidine **3**. An included water molecule on a crystallographic 2-fold axis, forms hydrogen bonds with the carboxylate–O atoms of two neighbouring complexed units. The hydrogen bonding arrangement does not extend beyond two units linked by water. The C–N bond lengths [1.306(3) and 1.324(3) Å] are short and similar, consistent with the formation of an amidinium salt.<sup>6b</sup> Similarly, the C–O bond lengths of **2** [1.259(2) and 1.269(2) Å] are typical for a carboxylate unit. The hydrogen atoms in the amidinium–carboxylate hydrogen bonds were found, and both are bound to the nitrogen atoms. The short N···O bond distances of 2.70 and 2.77 Å together with N–H···O angles of  $170^\circ$  and  $176^\circ$  indicate strong hydrogen bonds.<sup>6b,6c</sup> The (*E,E*) configuration of the

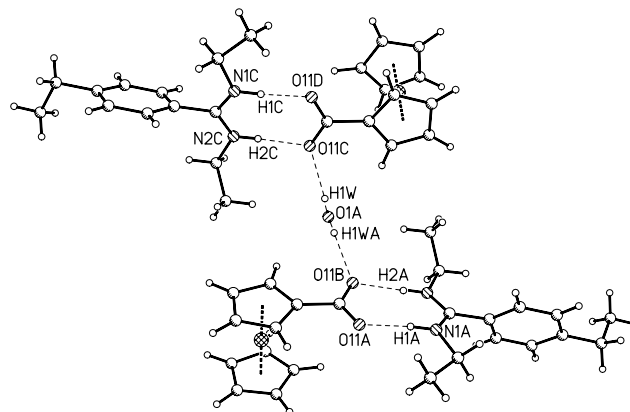


Figure 1. Crystal structure of complex **2**·**3**.

*N,N'*-diethyl-substituted amidinium group of complex **2**·**3** ensures that the binding interactions closely resemble those of unsubstituted amidines. However, the torsion angle between the amidine group and its adjacent benzene ring is  $64^\circ$ , due to the influence of the bulky *N,N'*-diethylamidinium group preventing planarity.<sup>6b,c</sup>

With salt bridge formation having been confirmed for **2**·**3** and **2**·**4** both in the solid state and in chloroform solution, we next investigated the role of electrochemistry to modulate binding in this supramolecular system using cyclic voltammetry (CV).<sup>7</sup> CV studies on compound **2** in  $\text{CH}_2\text{Cl}_2$  gave rise to a reversible single-electron oxidation at  $E_{1/2} = +0.81$  V. Addition of an excess of **3** or **4** to a solution of **2** resulted in a  $-0.27$  V ( $\pm 5$  mV) shift in the half-wave potential of the ferrocene derivative, indicating that salt bridge formation substantially lowers the oxidation potential of **2** (Fig. 2). This remarkably large negative shift corresponds to a considerable  $26$  kJ mol<sup>-1</sup> stabilisation of the ferrocenium state of **2**,<sup>8</sup> and is in accordance with the amidine becoming more strongly bound to **2**.<sup>9</sup> Interestingly, both amidines gave almost the same shifts in the half-wave

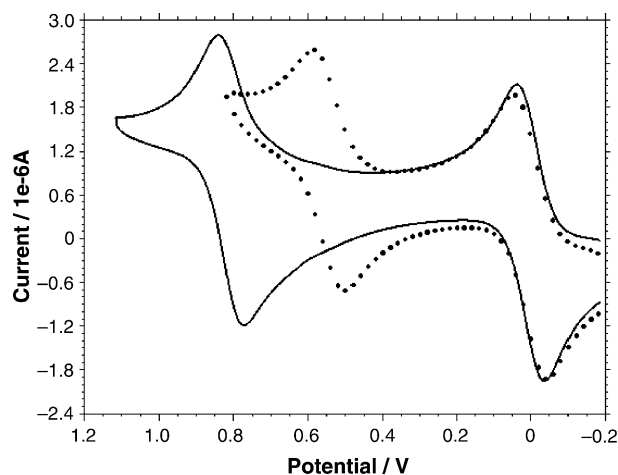
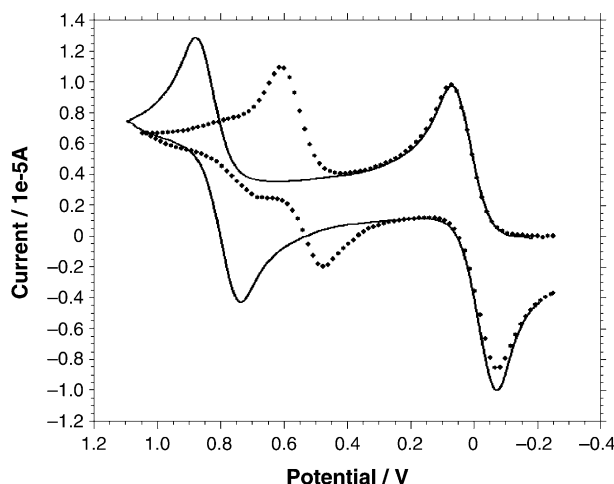


Figure 2. Cyclic voltammograms of a  $\sim 10^{-5}$  M solution of **2** in  $\text{CH}_2\text{Cl}_2$  (solid line) and after addition of excess ( $\sim 10^{-4}$  M) **4** (dotted line).

<sup>†</sup> Selected data for **2**·**3**: Yield 96%. Mp =  $95$ – $98^\circ\text{C}$ . IR (KBr)  $\nu$  3391, 3217, 2971, 1644, 1548, 1463, 1385,  $1344\text{ cm}^{-1}$ .  $^1\text{H}$  NMR (200 MHz,  $\text{CDCl}_3$ ):  $\delta$  12.8 (br s, 2H), 7.36, 7.19 (AA'XX',  $2 \times 2$  H, ArH amidine), 4.76, 4.21 (AA'XX',  $2 \times 2$  H, Cp), 4.20 (s, 5H, Cp), 3.02 (q,  $J$  7.1, 4H), 2.71 (q,  $J$  7.5, 2H), 1.27 (t,  $J$  7.5, 3H) 1.11 (t,  $J$  7.1, 6H). Anal. calcd for  $\text{C}_{24}\text{H}_{30}\text{FeN}_2\text{O}_2$ : C, 66.36; H, 6.96; N, 6.45. Found: C, 66.43; H, 7.08; N, 6.35.

Selected data for **2**·**4**: Yield 93%. Mp =  $104$ – $107^\circ\text{C}$ . IR (KBr)  $\nu$  3381, 3231, 3091, 2979, 1647, 1544, 1464, 1385,  $1343\text{ cm}^{-1}$ .  $^1\text{H}$  NMR (200 MHz,  $\text{CDCl}_3$ ):  $\delta$  7.71, 7.19 (AA'XX',  $2 \times 2$  H, ArH amidine), 4.76, 4.23 (AA'XX',  $2 \times 2$  H, Cp), 4.21 (s, 5 H, Cp), 3.03 (q,  $J$  7.1, 4H), 1.13 (t,  $J$  7.1, 6H). Anal. Calcd for  $\text{C}_{22}\text{H}_{25}\text{BrFeN}_2\text{O}_2$ : C, 54.46; H, 5.19; N, 5.77. Found: C, 54.53; H, 5.08; N, 5.88.

<sup>‡</sup> Selected crystal data for **2**·**3**:  $\text{C}_{24}\text{H}_{31}\text{FeN}_2\text{O}_{2.5}$ ,  $M = 443.36$ , monoclinic, space group,  $C2/c$ ,  $a = 26.9938(15)$  Å,  $b = 10.6994(6)$  Å,  $c = 16.9361(11)$  Å,  $\beta = 115.569(6)^\circ$ ,  $V = 4412.4(5)$  Å<sup>3</sup>,  $T = 160(2)$  K,  $Z = 8$ ,  $\mu = 0.708\text{ mm}^{-1}$ , 14,229 total reflections, 6383 unique [ $R(\text{int}) = 0.0533$ ],  $R = 0.0386$ ,  $wR = 0.0490$  for 2706 observed data [ $I > 2\sigma(I)$ ]. Intensity data were collected on a Xcalibur2 diffractometer at the Oxford Diffraction laboratory in Abingdon, Oxon. Crystallographic data for **2**·**3** have been deposited with the Cambridge Crystallographic Data Centre (CCDC reference number 209543).



**Figure 3.** Cyclic voltammograms of a  $\sim 9 \times 10^{-4}$  M solution of **2** (solid line) and a  $\sim 9 \times 10^{-4}$  M solution of **2·3** (dotted line).

potential of **2**, which is to be expected as the electronic influence of the substituents in the 4-position of the benzamidine is poorly communicated to the binding site, owing to the large torsion angle between the benzene ring and the amidinium group.

The CV data of the pure complex **2·3** has also been investigated.<sup>10</sup> A redox wave for the ferrocene unit was observed, which is shifted to a similar half-wave potential to that obtained when the CV data for **2** were recorded in the presence of an excess of the amidine. However, a more positive irreversible oxidation wave was also visible, which disappears upon the addition of excess amidine (Fig. 3). By comparing the intensity of peak currents of these waves to the one-electron oxidation wave of an equal concentration of decamethylferrocene internal standard, the sum of the two oxidation waves equate to a one-electron oxidation of the ferrocene unit. At low scan rates ( $25 \text{ mV s}^{-1}$ ), the more positive oxidation wave becomes more prominent, whilst at faster scan rates ( $10 \text{ V s}^{-1}$ ) this oxidation wave is less evident, and the more negative oxidation wave now prevails. We believe that the data are consistent with a slow dissociation of **2·3**, so that at slow scan rates two oxidation waves are detected for the complexed and free ferrocene unit. The more negative oxidation peak being due to **2·3**, whereas the peak at the more positive potential is due to an uncomplexed ferrocene unit. The redox wave for the latter process is shifted to a more negative potential compared to solutions of **2** alone, presumably due to a rapid recomplexation of **2** and **3** upon oxidation of the ferrocene unit.<sup>11</sup>

We have also recorded the voltammograms of **2** upon the addition of aliquots of **3** (Fig. 4). A new redox wave corresponding to the formation of the salt bridge gradually begins to appear upon the addition of the amidine, with a concomitant disappearance of the redox wave corresponding to free **2**. Interestingly, there is a gradual negative shift in the oxidation wave for the uncomplexed ferrocene unit following the addition of **3**. Furthermore,

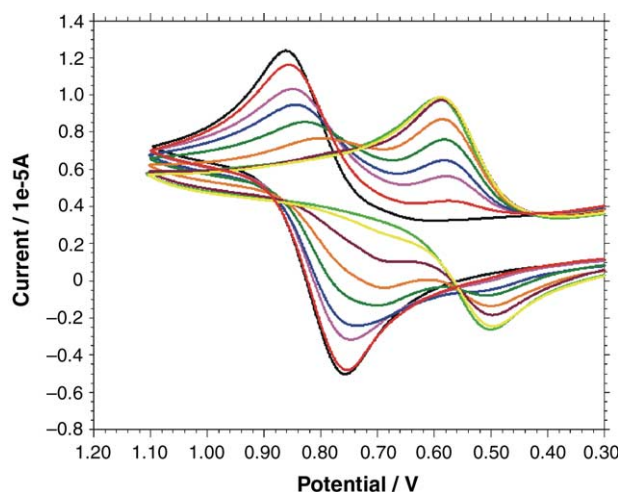


**Figure 4.** Cyclic voltammograms of a  $\sim 9 \times 10^{-4}$  M solution of **2** (—) and in the presence of approximately 0.2 (—), 0.4 (—), 0.6 (—), 0.8 (—), 1.0 (—), 1.2 (—), 1.4 (—) and 1.6 (—) equiv of **3**.

the redox wave formed at the more positive potential is not fully suppressed until more than 1 equiv (typically 1.2–1.4 equiv) of the amidine is added.

In conclusion, we have shown that proton transfer, which accompanies salt bridge formation between ferrocenecarboxylic acid and an amidine, results in a notable decrease in the oxidation potential of the ferrocene unit. Moreover, the large negative shift in the half-wave potential of **2** when the CV data were recorded in the presence of an excess of amidine, indicates a substantial stabilisation of the ferrocenium state of **2**, which is consistent with a significant increase in the hydrogen bonding efficiency of the **2·3** and **2·4** complexes. This result paves the way for the design of novel biomimetic systems that probe the role of proton and electron transfer in biological systems. Furthermore, as the binding efficiency rivals levels of redox enhancement previously only obtained by reductive processes, we have embarked on the development of electrochemically controlled devices that can be effectively actuated at positive potentials. Further electrochemical investigations of the redox behaviour of complexes **2·3** and **2·4** are underway, and the development of the biomimetic and device applications of related systems will be reported in due course.

### Acknowledgements

We gratefully acknowledge support from the EPSRC (studentship for FMAD), The EPSRC National Mass Spectrometry Service Centre, Swansea, The Royal Society, the Royal Society of Chemistry, the National Science Foundation (US) (VR) and Oxford Diffraction for crystallographic data collection. We thank Professor Fraser Armstrong for helpful discussions.

## References and Notes

1. For recent reviews containing aspects of supramolecular electrochemistry, see: (a) Kaifer, A. E.; Gómez-Kaifer, M. *Supramolecular Electrochemistry*; Wiley-VCH: Weinheim, 1999; (b) Boulas, P. L.; Gómez-Kaifer, M.; Echegoyen, L. *Angew. Chem., Int. Ed.* **1998**, *37*, 216; (c) Rotello, V. M.; Niemz, A. *Acc. Chem. Res.* **1999**, *32*, 44; (d) Kaifer, A. E. *Acc. Chem. Res.* **1999**, *32*, 62; (e) Tucker, J. H. R.; Collinson, S. R. *Chem. Soc. Rev.* **2002**, *31*, 147; (f) Cooke, G.; Rotello, V. M. *Chem. Soc. Rev.* **2002**, *31*, 275.
2. For examples of hydrogen-bonded host–guest complexes with binding efficiencies that increase upon electrochemical oxidation, see: (a) Carr, J. D.; Lambert, L.; Hibbs, D. E.; Hursthouse, M. B.; Malik, K. M. A.; Tucker, J. H. R. *Chem. Commun.* **1997**, 649; (b) Carr, J. D.; Coles, S. J.; Hursthouse, M. B.; Light, M. E.; Tucker, J. H. R.; Westwood, J. *Angew. Chem., Int. Ed.* **2000**, *39*, 3296; (c) Collinson, S. R.; Gelbrich, T.; Hursthouse, M. B.; Tucker, J. H. R. *Chem. Commun.* **2001**, 555; (d) Bourgel, C.; Boyd, A. S. F.; Cooke, G.; de Cremiers, H. A.; Duclairor, F. M. A.; Rotello, V. M. *Chem. Commun.* **2001**, 1954.
3. For examples of hydrogen-bonded host–guest complexes with binding efficiencies that increase upon electrochemical reduction, see: (a) Ge, Y.; Lilienthal, R. R.; Smith, D. K. *J. Am. Chem. Soc.* **1996**, *118*, 3976; (b) Ge, Y.; Miller, L.; Ouimet, T.; Smith, D. K. *J. Org. Chem.* **2000**, *65*, 8831; (c) Breinlinger, E.; Niemz, A.; Rotello, V. M. *J. Am. Chem. Soc.* **1995**, *117*, 5379.
4. For examples, see: (a) *Electron and Proton Transfer in Chemistry and Biology*; Müller, A., Ratajczaks, H., Junge, W., Diemann, E., Eds.; Elsevier: Amsterdam, 1992; (b) Ramirez, B. E.; Malmström, B. G.; Winkler, J. R.; Gray, H. B. *Proc. Natl. Acad. Sci. U.S.A.* **1995**, *92*, 11949; (c) Brzezinski, P. *Biochemistry* **1996**, *35*, 5611; (d) Okamura, M. Y.; Feher, G. *Ann. Rev. Biochem.* **1992**, *61*, 861; (e) Averill, B. *Chem. Rev.* **1996**, *96*, 2951; (f) Solomon, E. I.; Sundaram, U. M.; Machonchin, T. E. *Chem. Rev.* **1996**, *96*, 2563; (g) Burgess, B. K.; Lowe, D. J. *Chem. Rev.* **1996**, *96*, 2983.
5. (a) Chang, C. J.; Brown, J. D.; Chang, M. C. Y.; Baker, E. A.; Nocera, D. G. In *Electron Transfer in Chemistry*; Balzani, V., Ed.; Wiley-VCH: Weinheim, Germany, 2000; p 409, Chapter 3.2.4; (b) Nocera, D. G.; Cukier, R. I. *Ann. Rev. Phys. Chem.* **1998**, *49*, 337.
6. (a) Wulff, G.; Groß, T.; Schönfeld, R. *Angew. Chem., Int. Ed.* **1997**, *36*, 1962; (b) Kraft, A.; Peters, L.; Powell, H. R. *Tetrahedron* **2002**, *58*, 3499; (c) Peters, L.; Fröhlich, R.; Boyd, A. S. F.; Kraft, A. *J. Org. Chem.* **2001**, *66*, 3291.
7. All electrochemical experiments were performed using a CH Instruments 620A electrochemical workstation. The electrolyte solution (0.1 M) was prepared from recrystallised Bu<sub>4</sub>NPF<sub>6</sub> using spectroscopic grade CH<sub>2</sub>Cl<sub>2</sub>, and purged with nitrogen prior to use. A three-electrode configuration was used and consisted of a Pt working electrode, a silver wire pseudo-reference electrode and a platinum wire as the counter-electrode. Decamethylferrocene was used as internal standard, and the redox potentials are based upon the decamethylferrocene/decamethylferrocenium redox couple = 0 V. Scan rate = 100 mV s<sup>-1</sup> (unless otherwise stated). Temperature = 25 °C.
8. Calculated using:  $\Delta\Delta G = -nF\Delta E$ , where  $n$  is the number of electrons involved in process,  $F$  is the Faraday constant and  $\Delta E$  is the change in half-wave potential following complexation.
9. Previously, the association constant of protonated **3** and 4-methylbenzoate has been estimated to be >10<sup>6</sup> M<sup>-1</sup> in dry CDCl<sub>3</sub> at 25 °C: Wulff, G.; Schönfeld, R. *Adv. Mater.* **1998**, *10*, 957. Unfortunately, endeavours to obtain binding constants for our neutral host–guest complexes, and hence an estimation of the magnitude of redox-enhanced binding, were hampered by the hygroscopic nature of the tetrabutylammonium salt of **2**.
10. Similar electrochemical data were also observed for the **2-4** complex.
11. For electrochemical studies performed on ferrocene carboxylate, see: (a) De Santis, G.; Fabbri, L.; Licchelli, M.; Pallavicini, P. *Inorg. Chim. Acta* **1994**, *225*, 239; (b) Cassidy, J.; O’Gorman, J.; Ronane, M.; Howard, E. *Electrochem. Commun.* **1999**, *1*, 69.